

Inelastic scattering of neutrons by surface vibrations of highly disperse nickel

N. N. Besperstov, A. Yu. Muzychka, I. Natkaniec, P. B. Nechitaïlov, E. F. Sheka, and Yu. L. Shitikov

Patrice Lumumba University, Moscow

(Submitted 21 October 1988)

Zh. Eksp. Teor. Fiz. **96**, 1752–1763 (November 1989)

A difference method of inelastic incoherent neutron scattering (IINS) was used to obtain for the first time the vibration spectrum of highly disperse nickel at 80 and 300 K. An analysis of the experimental results showed that the IINS cross sections and the weighted functions representing densities of vibrational states of small particles deduced from them could be described in detail on the basis of the current ideas on the spectrum of vibrations of a thin plate. Three characteristic regions were identified and these represented true surface and mixed modes. The mixed mode region was most difficult to analyze. An adsorbate present on the surface of the particles was identified. The effects associated with the small particle size were considered.

1. INTRODUCTION

Small particles represent an intermediate state between a macroscopic solid and a molecule. They are difficult to treat theoretically so that an analysis of the experimental results is usually made by adopting one of two limits in which a small particle is either regarded as a solid with a large ratio of the surface area to the volume, with the properties dependent strongly on the surface, or it is treated as a giant molecule. The choice of the approach in any practical situation is determined, although not very rigorously, by the number of atoms N in a particle, on the other hand, and on whether a given property is collective or local, on the other. For example, vibrational properties of a particle consisting of $N \geq 10^5$ atoms can be quite reasonably discussed on the basis of solid-state physics. On the other hand, the processes of adsorption or desorption of atoms or molecules, governing in particular the heterogeneously catalyzed reactions on the surface, are due to the interaction with a small number of atoms in the substrate and are fully local. This is why they can be treated from the molecular point of view, irrespective of the particle size. If a particle itself consists of a small number of atoms ($N \leq 10^2$), it can be regarded as a quasimolecule and its electronic and vibrational properties can be described satisfactorily by the cluster approach (see, for example, Ref. 1).

We shall consider nickel particles with an average size 200–300 Å, which corresponds to $N \sim 10^5$. We shall be interested in the vibrational spectra, in the possibility of separating them into contributions of bulk and surface vibrations, and in a comparison with the spectra of bulk and surface phonon states in a massive sample.

The dispersion dependences and the density of the bulk phonon states of nickel have been investigated thoroughly both theoretically and experimentally (the latter by the inelastic neutron scattering method).² Since 1983, the dispersion dependences exhibited by surface phonon states in single crystals had been studied by the inelastic electron scattering method,³ known better as high-resolution spectroscopy of characteristic electron energy losses.⁴ The investigations carried out on nickel in the last five years have included detailed studies of the phonon states on a clean surface^{5,6} and on the surfaces covered by various adsorbates, primarily the “atmospheric” components, including oxygen,^{7,8} sulfur,⁹ hydrogen,^{10,11} water,^{12,13} nitrogen,¹⁴ and car-

bon monoxide.^{15,16} These thorough investigations of macroscopic samples provide a suitable basis for investigating the vibrational spectrum of microparticles of the same metal.

The disperse nature of a sample makes it possible to consider only the density of vibrational states and the best experimental method for investigating them is inelastic incoherent neutron scattering (IINS). The mean free path of a thermal neutron in matter is ~ 1 cm, so that an IINS spectrum is always a sum of the spectra representing the scattering of neutrons in the bulk of a sample and by surface atoms. In the case of a large sample (characterized by $N \gg 10^5$, which we shall call a macroscopic sample or macrosample) the contribution of the surface scattering is very small and, therefore, the IINS spectra can be used to determine the density of bulk phonon states. However, in the case of a sample with a large value of the surface-to-volume ratio s/v ($N \leq 10^5$, we shall call these microscopic samples) the contribution of the surface scattering can be considerable, as shown below. In this case again the scattering by surface vibrations can be determined experimentally by the difference method of IINS spectroscopy utilizing, for example, vibrational states of adsorbates on the surfaces of various substrates.¹⁷ This method involves determination, under identical conditions, of the IINS spectra for two samples, one of which is clean (“reference” sample) and the other coated by an adsorbate, and then finding the difference spectrum. The ability to use the difference IINS method to determine the spectrum of surface states of microscopic particles had been demonstrated earlier in the case of highly disperse powders of Ga (average molecule size 70–100 Å),¹⁸ TiN (~ 300 Å),¹⁹ and $\text{ZrO}_2 \cdot \text{Y}_2\text{O}_3$ (~ 190 Å).²⁰ The reference spectrum was in this case the spectrum of a macroscopic sample. We used this method for the first time to obtain the spectrum of surface states of a highly disperse metal.

2. SAMPLES AND EXPERIMENTAL METHOD

Highly disperse nickel (micro-Ni) was formed by electric pulse sputtering of a nickel wire of the NP-2 grade in an argon atmosphere; the composition of this wire was as follows: 99.8% Ni; 0.1% Fe; $\sim 0.01\%$ of Al and Cu; $\sim 0.02\%$ of Mg and Mn. An aerosol formed as a result of sputtering was deposited in an electrostatic filter collected in a capsule filled with argon. This argon was of the “extra” purity grade. Neutron¹ and x-ray diffraction investigations, carried out at

80 and 300 K, showed that the positions of the main peaks in the diffractograms of macroscopic and microscopic samples were basically identical. However, the diffractogram of the microscopic sample included additional peaks indicating the presence of $\sim 6\%$ of nickel oxide (NiO) and all the peaks were considerably broadened. The degree of this broadening was used to determine the average particle size, which was ~ 170 Å. Independent electron-microscopic investigations gave ~ 300 Å for the same average size. The specific surface area of the particles, deduced using calibrated physical adsorption of krypton,²¹ amounted to 22 m²/g, corresponding to an average particle size of ~ 250 Å. A discussion of the reasons for the difference between the dimensions found by different methods are outside the scope of the present paper. We therefore assumed that the average particle size was within the range 200–300 Å. In the temperature range from 300 to 600 K it was found that water and carbon monoxide were desorbed from the surface of a sample.²⁾ All these results were obtained for a sample which was not in contact with atmospheric air. Exposure to air did not alter its characteristics. Hence, the likely contamination, particularly the formation of an oxide, occurred during the preparation stages. A cassette used in the neutron scattering measurements was filled in atmospheric air. We used a rectangular cassette (184×164 mm), which was 4.5 mm thick. The mass of a microscopic sample was 55 g. The macroscopic sample of Ni of 99.97% purity was in the form of polycrystalline granules 6–8 mm in diameter and its mass was 914 g. A change in the ratio s/v due to the transition from a macroscopic to a microscopic sample amounted to 4×10^5 .

The IINS spectra of both samples were obtained under identical conditions at 80 and 300 K using a KDSOG-M spectrometer attached to an IBR-2 reactor at the Joint Institute for Nuclear Research, employing the time-of-flight method and the "reflection" positions corresponding to the scattering angles 80, 100, 120, and 140°. The IINS spectra were corrected by subtracting the background created by the cryostat and the cassette holding the sample. The measurements on a microscopic sample took 8 h (80 K) or 14.5 h (300 K), whereas in the case of a macroscopic sample the corresponding periods were 3.5 h (80 K) or 3.5 h (300 K); in each case the temperature is given here in parentheses.

Nickel used in the present study had the natural abundance of the isotopes. The coherent and incoherent neutron scattering cross sections were 13.3 and 5.2 barn, respectively. A sample was basically a coherent scatterer. However, the scattering was recorded at large angles, corresponding to the incoherent approximation. This made it possible to improve the statistics by combining the spectra obtained for different scattering angles. The combined spectra were normalized to 1 g of the mass of the powder and measurements for 1 h.

The observed $N(t)$ spectrum was a convolution of the scattering cross section with the instrumental function of the spectrometer and the spectrum of the incident neutrons.²² Assuming that the instrumental function was the δ function, we can find the scattering cross section from the simplified expression

$$\sigma(\omega) = N(t)/F(\omega, t) \quad (1)$$

where $F(\omega, t)$ is the spectrum of the incident neutrons. If the

scattering is a one-phonon incoherent process, the scattering cross section $\sigma^{(1)}(\omega)$ for a crystal with one atom in a unit cell is given by

$$\sigma^{(1)}(\omega) = \frac{k}{k_0} \frac{\hbar |\kappa|^2}{2\omega} |b|^2 W(\omega) \{n(\omega, T) + 1\} G(\omega), \quad (2)$$

where

$$G(\omega) = \frac{1}{M} \sum_j \int dQ |A_j(Q)|^2 \delta(\omega - \omega_j(Q)). \quad (3)$$

Here, k_0 and κ are, respectively the vectors of the incident and scattered neutrons and their difference; b is the scattering amplitude; M is the mass of an atom; $W(\omega)$ and $n(\omega, T)$ are the Debye–Waller factor and the occupancy number of a vibrational state of energy $\hbar\omega$, respectively; $G(\omega)$ is the weighted (using the square of the displacement of an atom A_j) density of vibrational states (WDVS); Q is the wave vector; j is the vibrational mode number. The relationships (1)–(3) were used by us in an analysis of the experimental spectra.

3. EXPERIMENTAL RESULTS

Figure 1 shows the normalized IINS spectra of macroscopic and microscopic samples of Ni. The experimental errors, representing the result-acquisition statistics, are represented by vertical segments. The influence of temperature is demonstrated in the case of microscopic samples of nickel (micro-Ni). The spectrum of macroscopic nickel (macro-Ni) was determined in a similar manner.

It is clear from Fig. 1 that the IINS spectrum changed considerably on transition from macro- to micro-Ni. The changes were not the same throughout the spectrum and, therefore, for convenience of analysis we split the IINS spectra in accordance with their characteristic structure into three regions labeled I, II, and III in Fig. 1. We shall first consider what these regions represent in the reference spectrum of a macrosample.

Figure 2 shows the function $G(\omega)$ deduced for macro-Ni in accordance with Eqs. (1)–(3). It also shows the calculated density of the phonon states in a crystal $g(\omega)$. It is clear from this figure that the experimental $G(\omega)$ spectrum is described quite satisfactorily by the function $g(\omega)$, which is typical of a monatomic crystal: two maxima in the main part of the spectrum represent the excitation of longitudinal and transverse acoustic waves. It follows from this figure that region I in the reference spectrum represents the long-wavelength acoustic modes typical of a crystal with the density described in the Debye approximation by $g(\omega) = \alpha\omega^2$. Region II is the main part of the one-phonon spectrum of a nickel crystal, which terminates at the boundary between regions II and III, so that weak scattering in region III may be attributed to the excitation of two-phonon states and multiple scattering.

A comparison of the spectra of macro- and micro-Ni (1 and 2 in Fig. 1) shows that at $T = 80$ K the scattering by micro-Ni is stronger than in the reference spectrum and this is true of all three regions. The same effect is observed also at $T = 300$ K. It is worth noting a singularity which occurs in the spectrum at $\omega = 137$ cm⁻¹ and is identified by an arrow in Fig. 1. At this point the scattering intensity recorded at $T = 80$ K is the same for both macro- and micro-Ni.

The changes in the scattering in these regions are manifested in different ways. In region I (0–140 cm⁻¹) the inten-

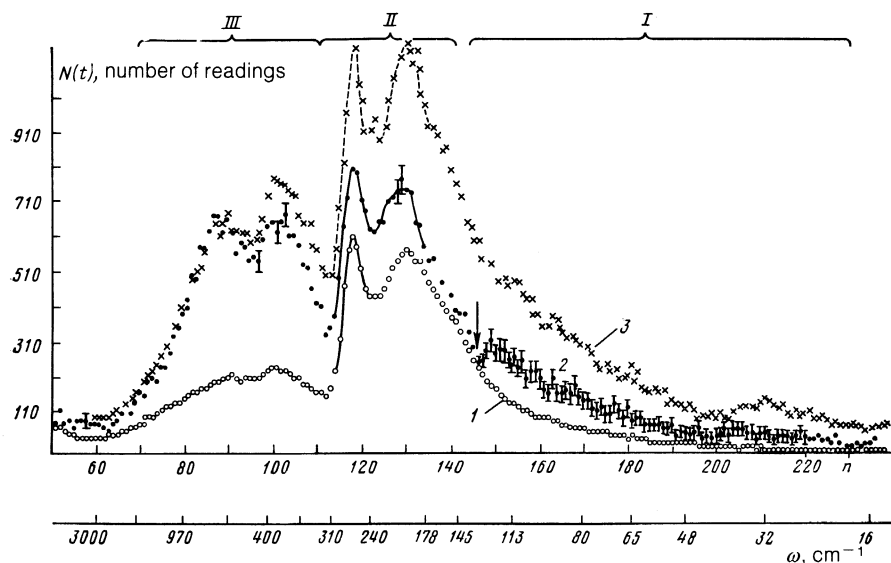


FIG. 1. Time-of-flight normalized inelastic neutron scattering spectra of powdered nickel: 1) macro-Ni, $T = 80$ K; 2) micro-Ni, $T = 80$ K; 3) micro-Ni, $T = 300$ K; n is the number of the time channel.

sity of the additional scattering is comparable with the intensity of the reference spectrum. This scattering spectrum is in the form of a wide band, superimposed on a monotonically rising part of the spectrum of macro-Ni which is a quadratic function of the frequency. In region II ($140\text{--}320\text{ cm}^{-1}$) the spectrum of micro-Ni is practically identical with the spectrum of the macroscopic sample. An increase in its intensity is on the average 30–40%, compared with the intensity in the reference spectrum. The greatest changes occur in region III ($320\text{--}2200\text{ cm}^{-1}$), where a new structured spectrum appears and the intensity is 3–4 times higher than the intensity of the scattering by the macrosample. Therefore, the main difference between the microsample and the macrosample is an increase in the ratio s/v by a factor of 10^5 and it is therefore natural to attribute the observed changes in the IINS spectrum to the excitation of surface vibrational states in a microscopic sample.

4. DISCUSSION OF RESULTS

The vibration spectrum of spherical particles of monatomic substances (such as metals and noble gases) has been investigated quite thoroughly (see Ref. 24 and the literature cited there). The attention has been concentrated on the dependences of the spectra on the particle size. It has been established that in the case of particles characterized by $N \gg 1000$ the vibrational spectrum is practically identical with that of a macrosample (a thin plate in Ref. 24). Since in our case we have $N > 10^3$, we shall analyze the recorded spec-

tra by comparing them with a spectrum of a thin plate characterized by a large value of the ratio s/v . This should make it possible to identify those regions in the IINS spectrum where bulk and surface vibrations predominate. The characteristics of the IINS spectrum are not explained by this procedure, and should be analyzed by considering the influence of the finite particle size on the spectrum.

The spectrum of harmonic vibrations of a thin plate consisting of an fcc monatomic metal has been investigated theoretically in detail^{25–28} for clean and adsorbate-coated nickel surfaces and is supported by recent experimental results obtained by the method of high-resolution characteristic energy loss spectroscopy.^{5,7,9,14,28,29} These results are used in Fig. 3 to show the overall structure of the spectrum of vibrations of nickel in the absence and presence of an adsor-

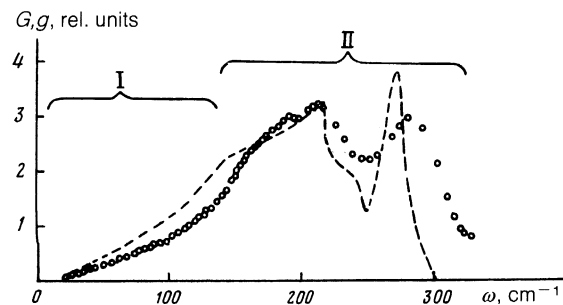


FIG. 2. Weighted density of the phonon states $G(\omega)$ of macro-Ni determined at $T = 80$ K (circles) and the calculated density of the phonon states $g(\omega)$ in a nickel crystal (dashed curve).²³

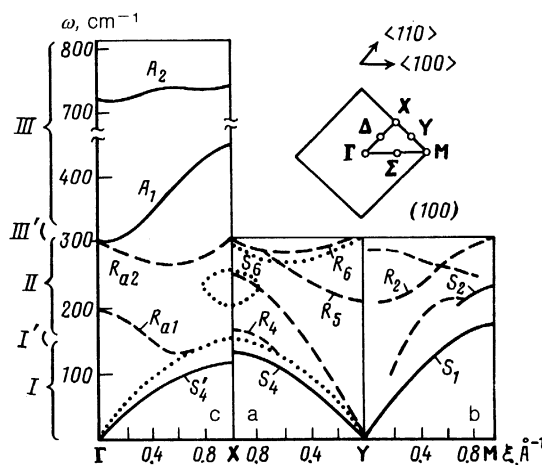


FIG. 3. Spectrum of the phonon states of a semi-infinite nickel crystal with the (100) surface. The calculation was carried out for a plate of thickness amounting to 21 atomic layers. The inset shows the two-dimensional Brillouin zone corresponding to the (100) surface. The reduced wave vector ξ for the ΓX and XY directions is $Q_{\parallel}/1.26\text{ \AA}^{-1}$ and for the YM direction it is $Q_{\parallel}/1.78\text{ \AA}^{-1}$. a), b) Spectra of phonons on the (100) surface of clean nickel along two directions in the two-dimensional Brillouin zone⁵; c) schematic representation of the spectrum plotted in accordance with the experimental results obtained by high-resolution characteristic energy loss spectroscopy applied to the $c(2 \times 2)N$ structure on the (100) surface of Ni (Ref. 14). The dotted curves are the boundaries of the spectrum of the bulk modes along the $\langle 110 \rangle$ crystallographic direction.

bate. It follows from the calculations that the spectrum of bulk vibrations of a thin plate is identical with the spectrum of a large sample. The spectrum of surface vibrations is quite complex (Figs. 3a and 3b). Type *S* modes represent vibrations within one layer of atoms (S_1 and S_4 for the first layer); the vibrations in the second layer are S_2 and S_6 , those in the third layer are S_7 and S_{10} , and in the fourth layer we have S_9 (Ref. 28); some of these vibrations corresponding to the $\langle 100 \rangle$ and $\langle 110 \rangle$ directions shown in Fig. 3 are true surface modes. Among them there is a low-frequency mode (S_4 and S_1 in Figs. 3a and 3b) representing a generalized Rayleigh wave and known as the Rayleigh mode.²⁶ Type *R* modes are resonant or mixed and they describe vibrational motion involving surface and bulk atoms. In the presence of an adsorbate there are also type *A* modes, representing vibrational motion in the adsorbate layer, and R_a modes combining the motion of adsorbate atoms with that of bulk atoms in the substrate.

An analysis of the structure of a vibrational spectrum reveals three characteristic regions: region I, located below the spectrum of bulk vibrations and containing mainly the Rayleigh mode, i.e., true surface modes of the substrate; region II representing mainly the spectrum of bulk vibrations of the substrate and of resonant modes (mixed state region); region III representing the vibrational spectrum of the adsorbate (true surface modes of the adsorbate). In addition to these regions there are two transition regions I' and III' with a complex structure of the spectrum. Separation of the vibration spectrum of a nickel single crystal with an adsorbate into three regions in Fig. 3 corresponds to the above separation of the experimental IINS spectrum in accordance with its characteristic structure. This makes it possible to analyze the experimental spectrum and identify its features.

High-frequency region of adsorbate vibrations

The existence of a strong IINS spectrum in the case of micro-Ni in the high-frequency region III (Fig. 1) is direct evidence of the presence of an adsorbate on the surface. The nature of the adsorbate can be identified by considering the difference spectrum in Fig. 4 representing the quantity $\Delta G(\omega) = G_{\text{micro}}(\omega) - G_{\text{macro}}(\omega)$, where the WDVS functions $G(\omega)$ are found from the experimental IINS spectra 1 and 2 using Eqs. (1)–(3).

As pointed out above, contamination of micro-Ni occurs during the stage of preparation and is clearly due to leakage of air into the chamber used during this stage and insufficient purity of gaseous Ar. We can therefore expect the adsorbates to be the components of the atmosphere. Shading is used in Fig. 4 to identify the regions of existence of the *A* modes of the atmospheric adsorbates on the surface of a single crystal of nickel deduced from the results obtained by high-resolution characteristic electron energy loss spectroscopy. We shall now arrange the components of the atmosphere in the decreasing order of their scattering cross section per elementary group of the adsorbate (estimates of the total cross sections in barns are given in the second line below):

$$\begin{array}{ccccccc} \text{H}_2\text{O} > \text{OH} > \text{H} > \text{Ni} > \text{CO} > \text{C} > \text{O} \\ 168 & 86 & 82 & 18,5 & 10 & 5,5 & 4,2 \end{array}$$

An analysis of the cross sections in this series shows that the high intensity of the difference spectrum should be at-

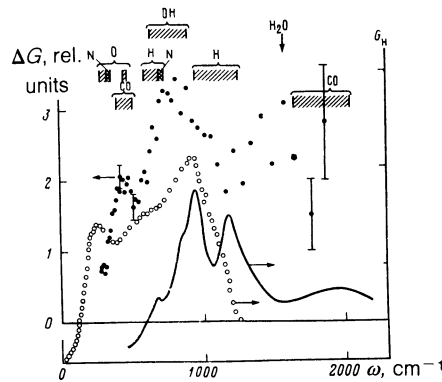


FIG. 4. Difference weighted density of the vibrational states of micro-Ni in region III, $T = 80$ K (black dots). The shaded regions are the results of high-resolution characteristic electron energy loss spectroscopy representing the intervals of the vibrational states of a number of adsorbates on (100) surface of nickel: H_2O (Refs. 12 and 13); O_2 (Refs. 7 and 8); S (Ref. 9); H_2 (Refs. 10 and 11); N_2 (Ref. 14); CO (Refs. 15 and 16). The continuous curve and the circles represent the IINS spectra of hydrogen adsorbed in the Raney nickel³⁰ and on deposited nickel catalyst.³¹

tributed primarily to adsorbates containing hydrogen (as confirmed by the release of water during desorption). In spite of the fact that hydrogen was observed only as water during desorption, it could be in one of three states: in an atomic state, or present in dissociatively adsorbed water

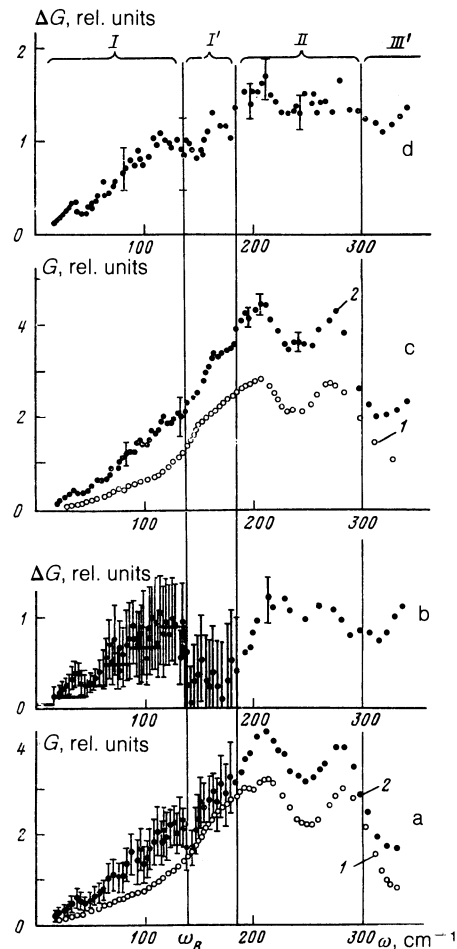


FIG. 5. Measured weighted densities of vibrational states $G(\omega)$ of nickel macro- and microsamples in regions I and II. a) $G(\omega)$ macro-Ni (1) and micro-Ni (2), $T = 80$ K; b) difference $\Delta G(\omega)$ spectrum, $T = 80$ K; c) same as a, $T = 300$ K; d) same as b, $T = 300$ K. The histogram represents the density of states of the Rayleigh mode for a plate 21 layers thick.³⁴

(forming hydroxyl radicals) or as molecularly adsorbed water. A comparison of the observed spectrum with the results obtained by high-resolution characteristic electron loss spectroscopy supported the presence of hydroxyl radicals. In fact, a smooth WDVS peak at 660 cm^{-1} coincided with a region corresponding to the vibrations of the Ni-O-H group.^{13,14} It is also well known that the presence of hydrogen on the nickel surface accelerates dissociation of water.¹³ The hydroxyl radical hypothesis is supported also by the observation that our spectrum did not exhibit the main features of the IINS spectra of atomic hydrogen adsorbed on other highly disperse catalysts such as the Raney nickel³⁰ or the G-17 catalyst deposited on an Al_2O_3 substrate³¹ (see Fig. 4). As to the molecular water, since the amount of desorbed water was considerable, some of the water could be adsorbed molecularly (for example, in the second layer) even on an oxidized surface. Indeed, we observed an "excess" WDVS in the region identified in Fig. 4 by an arrow and corresponding to characteristic bending vibrations of the water molecule.

A natural contaminant likely to be adsorbed on the surface of nickel was CO (see, for example, Refs. 5 and 10). The results obtained by high-resolution characteristic electron-energy-loss spectroscopy^{16,17} indicated that this adsorbate exhibited vibrational modes of the Ni-CO group in the region of $400\text{--}500\text{ cm}^{-1}$ and valence vibrations of CO in the region of $1700\text{--}2000\text{ cm}^{-1}$. The experimentally determined $\Delta G(\omega)$ spectrum showed clearly the maximum in the region of 420 cm^{-1} and fairly high values of the WDVS in the high-frequency region. Thus, the IINS data confirmed the results of desorption that a considerable amount of CO was present on the surface of micro-Ni and made it possible to identify the source of the desorbed water.

Range of energies of the mixed states ($140\text{--}320\text{ cm}^{-1}$)

The initial WDVS spectra [$G(\omega)$] of macro- and micro-Ni and the difference spectra $\Delta G(\omega)$, obtained in this region at two temperatures, are plotted in Fig. 5. The difference spectra $\Delta G(\omega)$ were quite strong at both temperatures (amounting to 30–40% of the spectrum of a macrosample) indicating a considerable change in the WDVS spectrum of the bulk vibrations. This could be due to modification of the vibrational spectrum [i.e., of $g(\omega)$], or due to changes in the nature of the motion of the atoms, i.e., due to an increase in A_j [see Eq. (3)].

Modification of the $g(\omega)$ spectrum undoubtedly occurred, because firstly—as demonstrated in Fig. 3—in this

part of the spectrum a considerable fraction of the density of the vibrational states was due to resonant mixed R and R_a modes and, secondly, in spite of the close similarity of the spectrum of the density of the vibrational states of a spherical particle with $N > 10^4$ to the spectrum of a large sample, calculations indicated a considerable difference in the region of the main maxima of the density of the vibrational states.²⁴ In the case of A_j the theory indicated that, firstly, on the whole the displacements of atoms in a small spherical particle, even one with $N > 100$, were greater than for atoms in a large sample³² and, secondly, the displacements of atoms in the course of excitation of the resonant modes were greater than in the excitation of the bulk modes and, thirdly and lastly, only 50% of the components of the displacement vector of the surface atoms was due to the true surface vibrations.³³ The remaining 50% represented the fraction of the volume modes which was reflected on reaching the surface. Consequently, the presence of such strongly scattering surface atoms as hydrogen should enhance the scattering by the bulk vibrations. Unfortunately, at this stage it was not possible to estimate the contribution made by each of these effects to the difference spectrum $\Delta G(\omega)$. Model theoretical calculations would be required.

Low-frequency range of the vibration spectrum

According to Fig. 3, the WDVS difference spectrum $\Delta G(\omega)$ obtained at low frequencies is mainly due to the Rayleigh mode and, therefore, it should be compared with the density of the states of this mode. Figure 5b shows a nominal calculated histogram of the density of states of the Rayleigh mode in the fcc lattice.³⁴ The density spectrum has a characteristic form: it consists of a monotonically rising function which reaches its maximum near the boundary of the two-dimensional Brillouin zone and falls strongly to zero at $\omega = \omega_R$; ω_R is the frequency of the Rayleigh mode at the boundary of this Brillouin zone. Thus in the case of a clean nickel surface the maximum value of ω_R is $\omega_R(\mathbf{M}) = 155\text{ cm}^{-1}$ (Ref. 5). Calculations give the following relationships between ω_R at the main high-symmetry points of the two-dimensional Brillouin zone²⁸: $\omega_R(\mathbf{X}) < \omega_R(\mathbf{M}) \sim \omega_R(\mathbf{K})$. The values of $\omega_R(\mathbf{X})$ and $\omega_R(\mathbf{M})$ were found by an investigation of the Ni (100 plane along the $\langle 110 \rangle$ and $\langle 100 \rangle$ directions, respectively (Fig. 3). Similarly, $\omega_R(\mathbf{M})$ and $\omega_R(\mathbf{K})$ could be determined by investigating the (111) plane along $\langle 211 \rangle$ and $\langle 110 \rangle$, respectively.²⁷ The deposition of an adsorbate of mass M_a less than or comparable with the mass of the

TABLE I. Frequency of the Rayleigh mode (cm^{-1}) at the boundary of the two-dimensional Brillouin mode of a nickel crystal.

Surface	High-symmetry points	ω_R		
		Calculation		Ref.
Ni(100)	M	155	155	[5]
	M	126; 141	—	[28]
	K	126; 149	—	[28]
	X	135	135	[5]
Ni(100) - c(2×2)S	X	111	113	[9]
Ni(100) - c(2×2)O	X	85	85	[7]
Ni(100) - p4mg(2×2)N	X	—	109	[14]
Ni(100) - p(2×1)H	X	—	135	[11]
Highly dispersed nickel + OH radicals and CO	Averaged over all high-symmetry points	—	137±5	Our results

metal M_m reduced ω_R , as demonstrated by high-resolution characteristic electron energy loss spectroscopy. Table I gives information on changes in ω_R on the (100) surface of nickel coated by various adsorbates.

Our experimental difference spectrum shown in Fig. 5b yielded the value ω_R amounting to $137 \pm 5 \text{ cm}^{-1}$ (the singularity in the spectrum 2 of Fig. 1 identified by an arrow corresponds precisely to this point). Naturally, this was the maximum value of ω_R in the spectrum of the Rayleigh mode of micro-Ni and it differed from the above maximum value for a single crystal. Assuming that the surface of a small particle was faceted in such a way that the main contribution to its structure came from the (111) planes, we found that the maximum value of ω_R was $\omega_R(\mathbf{M})$ so that the observed reduction in ω_R could indicate that ω_R was affected by the presence of the OH and CO adsorbates. However, if the main contribution to the structure of the surface came from the (100) plane, the observed value of ω_R was close to the maximum possible value of $\omega_R(\mathbf{X})$ and in this case we concluded that the adsorbate did not affect ω_R . Finally, the limiting frequency of the surface vibrations of a microparticle could differ from the maximum boundary frequency of the Rayleigh mode of a macrosample. The solution of this problem would require additional experimental and theoretical investigations.

In an analysis of the WDVS of the Rayleigh mode we observed an oscillatory structure of the density in this low-frequency region (Figs. 5b and 5d). This structure was observed at both temperatures, but it was clearer at $T = 80 \text{ K}$. The effect could be dimensional and associated with the transformation of a plane surface wave of the plate to a set of standing waves traveling along the surface of a spherical particle.²⁴ However, this conclusion would require a careful experimental check involving an investigation of the spectrum of the Rayleigh mode of particles of different sizes.

An analysis of Figs. 5a and 5b shows that, in addition to the regions I and II discussed above, the difference spectrum $\Delta G(\omega)$ included also regions I' and III' corresponding to the transition regions in Fig. 3c. The scattering in these two regions was due to the WDVS of the resonant modes split off below and above the spectrum of the bulk vibrations.

A comparison of the experimental WDVS difference spectrum $\Delta G(\omega)$ in regions I and II (Fig. 5b) with the calculated density of the surface states³⁴ indicated the absence of negative regions in the spectrum of the bulk states (region II), which should compensate the splitting of the surface modes in the $g(\omega)$ spectrum. This could be explained by assuming that in the observed WDVS spectrum $G(\omega)$ a reduction in the density of states $g(\omega)$ was compensated by an increase (compared with the macrosample) of the amplitudes of the displacements of atoms on excitation of the bulk and resonant modes because of the participation of the surface atoms (including those of the hydrogen-containing adsorbate) in these vibrations. Further experiments on micro-Ni with a clean surface and coated with other adsorbates could provide more specific information on this topic.

Temperature effects

An increase in the temperature of a sample from 80 to 300 K resulted in major changes in the $G(\omega)$ spectrum of micro-Ni compared with macro-Ni (Figs. 5a and 5c). The anharmonic effects in the spectrum of the bulk vibrations of

a nickel crystal were relatively weak and reduced to a slight softening of the phonon spectrum and the resultant redistribution of the density of states $g(\omega)$ (Ref. 23). It is clear from Figs. 5b and 5d that in the case of the microsample the main changes on increase in temperature occurred in region II, where the excess WDVS increased by a factor of about 1.5, but there was little change in the profile. An increase in temperature had practically no effect on the profile or intensity of the spectrum $\Delta G(\omega)$ in region I. This was also true of the $\Delta G(\omega)$ spectrum in region III. Therefore, the observed temperature effect resulted in a considerable increase in the intensity of the $\Delta G(\omega)$ spectrum on increase in temperature only in region II. This effect could be explained by assuming that the anharmonicity of the surface states was largely due to the mixed modes and this was manifested by a considerable increase on increase in the temperature of the amplitude of the displacements of the atoms on excitation of these vibrations.

An increase in these amplitudes and softening of the spectrum of the bulk modes as a result of an increase in the temperature of a sample accounted also for the apparent shift of the emitting frequency ω_R of the Rayleigh mode and of the spectrum of the split resonant modes (region I') toward higher frequencies and an increase in the intensity in this region because of a shift of the WDVS of the mixed modes in the difference spectrum toward lower frequencies increased the overlap of regions I and II.

5. CONCLUSIONS

The IINS difference spectroscopy method yielded for the first time the spectrum of the surface vibrations of highly disperse nickel in the range 0–2000 cm^{-1} . An analysis of the IINS spectra of small particles and of the WDVS spectra deduced from them can be described satisfactorily on the basis of the current ideas on the structure of the vibrational spectrum of a thin plate. The existence of three characteristic regions located below, inside, and above the spectrum of the bulk vibrational states was established. Outside the spectrum of the bulk states the vibrations were truly of the surface nature and were associated with the motion of the metal and adsorbate atoms in the low- and high-frequency regions, respectively. The most difficult to analyze qualitatively and quantitatively was the region coinciding with the spectrum of the bulk vibrations.

Not underestimating the value of the results obtained by high-resolution characteristic electron energy loss spectroscopy, without which the behavior of the surface phonons could not have been determined, we may conclude that the IINS difference method provides new opportunities which supplement significantly the results obtained from the characteristic loss spectra. In investigations made by the method of high-resolution characteristic electron energy losses the quantity obtained is the spectral density of the vibrational states⁵ or the density of the states weighted using the square of the normal component of the dipole moment:

$$\rho_{\beta\beta'}(\mathbf{Q}_{\parallel}) = \sum_j P_{\perp\beta}^j(\mathbf{Q}_{\parallel}) P_{\perp\beta'}^{*j}(\mathbf{Q}_{\parallel}) \delta(\omega - \omega_j(\mathbf{Q}_{\parallel})), \quad (4)$$

where $P_{\perp\beta}^j(\mathbf{Q}_{\parallel})$ is the component of the dipole moment normal to the surface and due to the β th component of the polarization vector of the j th vibrational mode of frequency $\omega_j(\mathbf{Q}_{\parallel})$ corresponding to a given value of the component of

the wave vector Q_{\parallel} parallel to the surface. The special nature of the spectral density of Q_{\parallel} is the basis for determination of the dispersion curves. The IINS difference is related to the total vibrational spectrum. By analogy with the coherent and incoherent neutron scattering results which made it possible to establish a quantitative theory of the bulk phonon spectrum of crystals, high-resolution characteristic electron energy loss spectroscopy and the difference IINS spectra are now making it possible to establish a similar theory for surface states. This approach has already been implemented in the case of high-resolution characteristic electron energy loss spectroscopy, whereas the potentialities of the difference IINS spectroscopy of small particles demonstrated in the present paper should provide a stimulus for the development of a quantitative theory of neutron spectroscopy of such particles.

¹¹We take this opportunity to thank A. V. Burkhanov and V. F. Petrunin from the Moscow Engineering-Physics Institute for neutron diffraction analysis.

¹²Physicochemical investigations were carried out by A. B. Kuznetsova and by V. V. Losev from the Institute of Chemical Physics of the USSR Academy of Sciences, to whom the authors are grateful for this help.

¹J. A. A. J. Perenboom and P. Wyder, *Phys. Rep.* **78**, 173 (1981).

²R. J. Birgeneau, J. Cordes, G. Dolling, and A. D. B. Woods, *Phys. Rev.* **136**, A1359 (1964).

³S. Lehwald, J. M. Szeftel, H. Ibach, *et al.*, *Phys. Rev. Lett.* **50**, 518 (1983).

⁴T. S. Rahman, J. E. Black, and D. L. Mills, *Phys. Rev. B* **25**, 883 (1982).

⁵M. Rocca, S. Lehwald, H. Ibach, and T. S. Rahman, *Surf. Sci.* **171**, 632 (1986).

⁶S. Lehwald, F. Wolf, and H. Ibach, *J. Electron Spectrosc. Relat. Phenom.* **44**, 393 (1987).

⁷J. M. Szeftel, S. Lehwald, H. Ibach, *et al.*, *Phys. Rev. Lett.* **51**, 268 (1983).

⁸K. G. Lloyd and J. C. Hemminger, *Surf. Sci.* **143**, 509 (1984).

⁹S. Lehwald, M. Rocca, H. Ibach, and T. S. Rahman, *Phys. Rev. B* **31**, 3477 (1985).

¹⁰P. A. Karlsson, A. S. Martensson, S. Andersson, and P. Norlander, *Surf. Sci.* **175**, L759 (1986).

¹¹H. Ibach, S. Lehwald, and B. Veigtländer, *J. Electron Spectrosc. Relat. Phenom.* **44**, 263 (1987).

¹²M. Hock, U. Seip, I. Bassignana, *et al.*, *Surf. Sci.* **177**, L978 (1986).

¹³C. Benndorf, C. Nöbl, and T. E. Madey, *Surf. Sci.* **138**, 292 (1984).

¹⁴W. Daum, S. Lehwald, and H. Ibach, *Surf. Sci.* **178**, 528 (1986).

¹⁵H. Lindner, D. Rupperecht, L. Hammer, and K. Müller, *J. Electron. Spectrosc. Relat. Phenom.* **44**, 141 (1987).

¹⁶L. Westerlund, L. Jönsson, and S. Andersson, *Surf. Sci.* **199**, 109 (1988).

¹⁷R. R. Cavanagh, J. J. Rush, and R. D. Kelley, in: *Vibrational Spectroscopy of Molecules on Surfaces* (ed. by J. T. Yates, Jr. and T. E. Madey), Plenum Press, New York (1987), p. 183.

¹⁸V. N. Bogomolov, N. A. Klushin, N. M. Okuneva, *et al.*, *Fiz. Tverd. Tela (Leningrad)* **13**, 1499 (1971) [*Sov. Phys. Solid State* **13**, 1252 (1971)].

¹⁹K. H. Rieder and W. Drexel, *Phys. Rev. Lett.* **34**, 148 (1975).

²⁰O. E. Zoteev, P. G. Ivanitskiĭ, S. A. Nepiĭko, and K. V. Chuistov, *Poverkhnost'* No. 3, 154 (1985).

²¹A. V. Kiselev and V. P. Dreving (eds.), *Experimental Methods in Adsorption and Gas Chromatography* [in Russian], Moscow State University (1983).

²²E. L. Bokhenkov, I. Natkaniec, and E. F. Sheka, *Zh. Eksp. Teor. Fiz.* **70**, 1027 (1976) (*Sov. Phys. JETP* **43**, 536 (1976)).

²³G. A. de Wit and B. N. Brockhouse, *J. Appl. Phys.* **39**, 451 (1968).

²⁴A. Tamura and T. Ichinokawa, *J. Phys. C* **16**, 4779 (1983).

²⁵R. E. Allen, G. P. Alldredge, and F. W. de Wette, *Phys. Rev. B* **4**, 1648 (1971).

²⁶R. E. Allen, G. P. Alldredge, and F. W. de Wette, *Phys. Rev. B* **4**, 1661 (1971).

²⁷G. P. Alldredge, R. E. Allen, and F. W. de Wette, *Phys. Rev. B* **4**, 1682 (1971).

²⁸J. E. Black, F. C. Shanes, and R. F. Wallis, *Surf. Sci.* **133**, 199 (1983).

²⁹B. M. Hall and D. L. Mills, *Phys. Rev. B* **34**, 8318 (1986).

³⁰H. Jobic, G. Clugnet, and A. Renouprez, *J. Electron. Spectrosc. Relat. Phenom.* **45**, 281 (1987).

³¹R. Stockmeyer, H. Stortnik, I. Natkaniec, *et al.*, *Ber. Bunsenges. Phys. Chem.* **84**, 79 (1980).

³²R. E. Allen and F. W. de Wette, *J. Chem. Phys.* **51**, 4820 (1969).

³³A. Tamura, K. Higeta, and T. Ichinokawa, *J. Phys. C* **16**, 1585 (1983).

³⁴D. L. Mills, *J. Electron. Spectrosc. Relat. Phenom.* **44**, 239 (1987).

Translated by A. Tybulewicz